

# Journal Pre-proofs

Research papers

Managed Phreatic Zone Recharge for Irrigation and Wastewater Treatment

DWS Tang, SEATM Van der Zee, DM Narain-Ford, GAPH van den Eertwegh, RP Bartholomeus

PII: S0022-1694(23)01150-2  
DOI: <https://doi.org/10.1016/j.jhydrol.2023.130208>  
Reference: HYDROL 130208

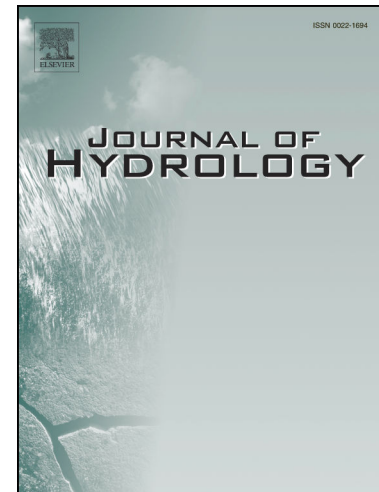
To appear in: *Journal of Hydrology*

Received Date: 24 April 2023  
Revised Date: 27 August 2023  
Accepted Date: 31 August 2023

Please cite this article as: Tang, D., Van der Zee, S., Narain-Ford, D., van den Eertwegh, G., Bartholomeus, R., Managed Phreatic Zone Recharge for Irrigation and Wastewater Treatment, *Journal of Hydrology* (2023), doi: <https://doi.org/10.1016/j.jhydrol.2023.130208>

This is a PDF file of an article that has undergone enhancements after acceptance, such as the addition of a cover page and metadata, and formatting for readability, but it is not yet the definitive version of record. This version will undergo additional copyediting, typesetting and review before it is published in its final form, but we are providing this version to give early visibility of the article. Please note that, during the production process, errors may be discovered which could affect the content, and all legal disclaimers that apply to the journal pertain.

© 2023 Published by Elsevier B.V.



1 **Managed Phreatic Zone Recharge for Irrigation and**  
2 **Wastewater Treatment**

3 **DWS Tang<sup>1</sup>, SEATM Van der Zee<sup>1</sup>, DM Narain-Ford<sup>2,3,4,5</sup>, GAPH van den Eertwegh<sup>6</sup>, RP**  
4 **Bartholomeus<sup>1,2</sup>**

5

6

7 1. Soil Physics and Land Management, Wageningen University, Wageningen, the Netherlands

8 2. KWR Water Research Institute, Nieuwegein, the Netherlands

9 3. Copernicus Institute of Sustainable Development, Utrecht University, Utrecht, the Netherlands

10 4. Institute for Biodiversity and Ecosystem Dynamics, University of Amsterdam, Amsterdam, the  
11 Netherlands

12 5. Centre for Sustainability, Environment and Health, National Institute for Public Health and the  
13 Environment (RIVM), Bilthoven, The Netherlands

14 6. KnowH2O, Berg en Dal, the Netherlands

15

16

17

18

19 **Abstract**

20 Managed phreatic zone recharge with marginal water, using (existing) drainage systems, raises the  
21 water table and increases water availability for crops. This is a newly developed method of freshwater  
22 conservation and marginal water treatment and disposal, but risks crop and environmental  
23 contamination. The fate of contaminants of emerging concern (CECs) within the irrigated water is  
24 addressed. We introduce numerical and analytical models, inspired loosely by a field site where treated  
25 domestic wastewater is used for subsurface irrigation. The treated wastewater would otherwise have  
26 been discharged into rivers, thereby spreading downstream. Model results show that minimal amounts of  
27 CECs are transported to deeper aquifers. Crops are not contaminated, except during dry years where  
28 small amounts of mobile CECs rise to the root zone, but then only directly above each irrigation drain.  
29 Under an annual precipitation surplus, less-mobile solutes are thus unlikely to ever enter the root zone.  
30 The primary mechanism of solute transport is lateral advection within the phreatic aquifer. Despite  
31 spatio-temporal heterogeneity in water flux magnitudes and directions, contaminant retardation does not  
32 significantly alter mass balance outcomes, only how fast it gets there. Therefore, persistent CECs pose  
33 the greatest risks, though overall environmental and crop contamination risks appear low. To maximize  
34 complementarity with subsurface irrigation systems, future advances in water treatment technologies  
35 should focus on removing persistent CECs. However, the system may be unsuitable for climates with  
36 annual precipitation shortages, as CECs may accumulate in the root zone and crops.

37

38 **Keywords:**

39 Groundwater aquifer; Irrigation and drainage; Contaminant transport; Wastewater reuse; Bioremediation

40

41 **Highlights:**

42 New subsurface irrigation and drainage method that raises the phreatic water table.

43 New method synergistic with marginal water irrigation: crops not directly exposed.

44 Tool for irrigation, freshwater conservation, and wastewater treatment and disposal.

45 Crop contamination risk is low, except by mobile contaminants in very dry years.

46 Crop and wider environmental contamination risk largest for persistent contaminants.

**1. Introduction**

Even in temperate humid regions, periodic shortages of fresh water resources may constrain irrigation. Use of treated wastewater for irrigation may be an effective strategy to balance regional fresh water supply and agricultural water demand (Dingemans et al., 2021; Pronk et al., 2021; Narain-Ford et al., 2021). Water stress caused by climate change exacerbates the need to re-use treated wastewater (Elliott et al., 2014). Moreover, the treated wastewater may contain nutrients, which enriches the soil (Lubello et al., 2004). However, wastewater treatment does not remove all impurities from the water, such as pharmaceuticals, pathogens, and other contaminants of emerging concern (CECs) (Yang et al., 2017; Richardson and Ternes, 2018). Surface irrigation with treated wastewater may cause adverse health effects amongst farm workers and the general public through direct exposure or crop contamination (Qadir et al., 2010; Devaux et al., 2001). It may also adversely affect soil fertility because it induces nutrient leaching (Dole et al., 1994) and alters the pH and composition of root zone water (Mohammad and Mazahreh, 2003). Meanwhile, treated industrial and domestic wastewater is often discharged via surface water channels towards the sea, spreading contaminants along these discharge paths (Beard et al., 2019). Accordingly, utilizing treated wastewater in subsurface irrigation may reduce these risks (Narain-Ford et al., 2020). An estimate of the potential of subirrigation for the Netherlands shows that it is logistically plausible for 78% to 84% of all treated wastewater to be used in subirrigation, which would reduce freshwater demand in agriculture by 8% to 12% (Narain-Ford et al., 2021).

65

Subsurface irrigation and drainage of phreatic aquifers using marginal water as water supply, is a new irrigation and drainage technology that allows for treated wastewater to undergo further in-situ filtration and remediation in the soil, while simultaneously ameliorating crop water stress and freshwater scarcity (Narain-Ford et al., 2022). Subirrigation is applied using controlled drainage systems, which can drain excess water (prevent waterlogging) and recharge the phreatic aquifer (subirrigation) when necessary. In this system, subirrigation pipes are buried in the phreatic zone some distance below the root zone. Therefore, the irrigation raises the water table. The CEC-free soil moisture located between the pipes and the root zone then rise towards the root zone due to capillary rise, and the effluent does not enter the root zone directly (Bern et al., 2013). Controlled drainage may also reduce nutrient losses from the root zone caused by high groundwater levels (Bonaiti and Borin, 2010; Peng et al., 2015; Borin et al., 2001; Borin et al., 1998), and reduce the spreading of the CECs contained in the effluent. Buried pipes that are already widely present in agricultural fields for the purpose of drainage (De Wit et al., 2022) may be used for subirrigation, making this a potentially low-cost and accessible option.

79

Irrigation from the subsurface rather than the surface aims to minimize direct crop exposure to CECs. This nature-based solution uses the soil, groundwater, and rainwater between the drains and root zone as a buffer zone for biodegradation and adsorption, similar to river bank filtration and constructed wetlands (Narain-Ford et al., 2020). Due to biodegradation and adsorption, the soil functions as a bioreactor. Due to these processes and dilution, water recovered by the drains during wet periods may contain lower concentrations of CECs than the injected effluent, and thereby be of higher quality. This improved water may be used instead of freshwater for some appropriate purpose, such as industrial processes, thus further conserving freshwater. Many CECs, being organic compounds, are biodegradable to some extent by soil microbes, both in the unsaturated (Bekele et al., 2011) and saturated (Rauch-Williams et al., 2010) zones. However, there is still a large uncertainty in the biodegradation rate and extent (Greskowiak et al., 2017). Persistent CECs may enter the root zone through dispersion and capillary rise, or be advected further into the environment by groundwater flow. With subsurface irrigation, the exposure of crops to CECs is indirect, and the groundwater is directly exposed, which is opposite to traditional surface irrigation systems. Therefore, it is important to investigate the risks of both crop and environmental contamination specific to subirrigation systems.

95

In this paper we construct numerical and analytical models to investigate effluent transport in the subsurface and the risks of crop and environmental contamination with CECs in subirrigation systems. We build upon a controlled drainage and subsurface irrigation system fed with treated domestic wastewater, that has been implemented in the Netherlands and monitored since 2015 (Narain-Ford et al., 2022). Solute fate is modelled for tracers and a reactive solute sampled during the experiment. These results may be translated to other hydrogeological properties and CEC types by varying the parameters in the model. We emphasize that the models constructed here are not meant to recreate the field site, but rather, meant to illustrate the fate of CECs in a generic controlled drainage-subirrigation system that represents a simplified concept of the field experiment, in climatic conditions typical of the Netherlands. The simple and generic nature of the models would better elucidate physical processes

106 governing contaminant fate, and allow it to be more easily adapted to other implementations of the  
107 system. Some data from the field experiment is presented in this study as it serves as proof-of-concept,  
108 to show that the model created is able to generally account for the important physical processes that  
109 govern solute transport and fate, particularly mass balances, in a generic subsurface irrigation and  
110 drainage system.

111

112 With the models, the processes that affect the fate of solutes contained within the effluent (tracers and  
113 geochemically reactive CECs that undergo adsorption and biodegradation) are characterized. Solute mass  
114 balances, breakthrough curves, and plume transport behavior are analyzed. Partitioning of solute fate is  
115 between crop solute uptake, advection in the phreatic groundwater, leaching to deeper groundwater,  
116 biodegradation, soil water, and drainage by the drainage system. The partitioning of the fate of irrigated  
117 solute mass (i.e. the relative solute mass balance) ultimately determines the extent of crop and  
118 environmental contamination. Furthermore, we also use the model to investigate the potential of the  
119 subirrigation system to lead to adverse environmental effects in the long-term, such as long-term  
120 accumulation of CECs in the soil. Hence, the model reveals aspects of the system that cannot be  
121 obtained from available experimental data, such as a more extensive spatio-temporal characterization of  
122 CEC transport processes, suitability of the system under different climates and hydrological conditions,  
123 the potential for CEC transport to deeper aquifers and surface water, and the risk of crop uptake of CECs.

124

## 125 **2 Methods**

### 126 **2.1 Field site**

127 The subsurface irrigation and drainage system we use as an example is implemented in a 58500 m<sup>2</sup> field  
128 site in Haaksbergen, the Netherlands, and is the only such system in operation. Maize grain destined to  
129 be livestock fodder is grown. Treated wastewater from a domestic wastewater treatment plant is fed into  
130 the subsurface irrigation and drainage system, which has been in operation since May 2015. Further  
131 details of the field site are available in detail in Narain-Ford et al (2022), and will not be reproduced  
132 here.

133

### 134 **2.2 Hydrogeological model**

135 The subsurface irrigation/drainage system was modeled with HYDRUS-2D (Šimůnek et al., 2016). Many  
136 studies in the literature have shown that HYDRUS-2D is suitable for simulating subirrigation (Cai et al.,  
137 2019; Saefuddin et al., 2019; Siyal et al., 2013) and drainage (Kacimov and Obnosov, 2021) systems.  
138 For brevity, a description of HYDRUS-2D will not be reproduced here. An overview of the parameter  
139 values and the sources they were obtained from can be found in Table 1. Some hydrogeological  
140 parameters (Table 1) were calibrated by comparing groundwater levels simulated without irrigation and  
141 crops, against field data obtained from a grassfield 1km from the experimental plot, with a post-  
142 calibration Nash-Sutcliffe efficiency of 0.61 (Figure 1), which is considered good (Moriassi et al., 2007).  
143 The subsurface soil and phreatic aquifer is simulated to a depth of 4m, as the two sampled tracer types  
144 were not detected beneath that level in six years of experimental data (Figure 2). Furthermore, borehole  
145 soil profiling has revealed that a poorly conductive loam layer is present at 4m depth at the middle of the  
146 experimental site.

147

148 We construct a 13m by 4m model domain (Figure 3a) to represent the subsurface to a depth of 4m from  
149 the soil surface, with a root zone of the maize crop that reaches a depth of 0.6m, and two  
150 drainage/irrigation pipes buried 1.2m beneath the surface spaced 6m apart. We insert breakthrough  
151 curve observation points at the same approximate locations as in the field experiment (0.2m, 0.6m,  
152 1.0m beneath the soil surface, and 0.25m, 0.8m, 1.3m beneath drain level), with one column of  
153 observation points directly above and below the downstream irrigation drain, and one column midway  
154 between the two drains, for a total of twelve points.

155

156 The top boundary for water flow is an atmospheric boundary that represents precipitation; excess  
157 precipitation beyond the soil's infiltration capacity is lost to runoff (Šimůnek et al., 2016). Daily

158 precipitation and reference evapotranspiration data (calculated according to Makkink, 1957) were  
 159 obtained from the Dutch meteorological institute (KNMI). The daily potential evapotranspiration of the  
 160 root zone during the crop season was calculated by multiplying the reference evapotranspiration with a  
 161 weekly crop factor for Dutch grain maize crops (LAGO, 1984). Outside of the crop season, the reference  
 162 evapotranspiration was used as the potential evapotranspiration. These atmospheric fluxes are shown in  
 163 Figure S1 in the supplementary material. The root distribution, which controls the spatial distribution of  
 164 root water uptake, is modelled with a maximum intensity at depth  $z = 0.05\text{m}$  (the first root zone layer in  
 165 Figure 3b), and thereafter a decreasing intensity in the following three root zone layers, with relative  
 166 intensities 8,4,2,1. The potential evapotranspiration rate is partitioned across each node in the root zone  
 167 proportionally to the root density at each node (Šimůnek and Hopmans, 2009). The actual root water  
 168 uptake flux is then determined with the pressure head reduction function of Feddes et al (1978), with the  
 169 parameters for corn (Wesseling et al, 1991) that are pre-programmed into Hydrus 2D.

170

171 Each irrigation drain is modelled as a circular opening with a 4cm internal diameter and 8cm external  
 172 diameter. The crop season in the model lasts for 150 days every year starting from the first of May, while  
 173 the drainage season occurs the rest of the time. The irrigation drains have imposed pressure head  
 174 boundaries during the crop season, and 'seepage face' boundary conditions (Liu et al., 2021) outside the  
 175 crop season. The bottom boundary is a deep drainage boundary condition: an imposed flux boundary  
 176 whose magnitude depends on the groundwater level (Hopmans and Stricker, 1989) according to the  
 177 formula  $q = A \exp(B|h - Z|)$  m/day, where  $h$  is the hydraulic head at the boundary, and  $A, B, Z$  are empirical  
 178 constants. The left (upstream) boundary for water flow is an imposed head gradient boundary  
 179 representing the regional head gradient. The right (downstream) boundary is a Cauchy boundary  
 180 condition comprised of a prescribed head and prescribed conductivity different from the rest of the  
 181 aquifer.

182

183 The initial conditions for water flow were set to hydrostatic equilibrium relative to a water table depth of  
 184 1m, corresponding to measurement data from the unirrigated field on the day before the crop season of  
 185 2016 began. Initial conditions for solutes were set as the rainwater concentration at the top boundary,  
 186 the groundwater concentration at the bottom boundary, and a linear distribution with depth within the  
 187 model domain. The simulation period of the model is four years, starting from the crop season of 2016.

188

189 The regional groundwater head gradient has a large and direct effect on solute breakthrough curves,  
 190 especially at the observation points located at a larger distance from the drains. This is caused by the  
 191 direct impact of regional groundwater head on the lateral advection velocity, and because it is  
 192 responsible for a much larger proportion of the flux passing through the simulated domain than any  
 193 other flux source or sink. Since detailed information on the regional head gradient over the measurement  
 194 period is unavailable, the regional head gradient also has a significant contribution to uncertainty in the  
 195 model parameterization. The combination of relatively large uncertainty in a relatively impactful  
 196 parameter might manifest as uncertainty in the simulation results. To identify the extent to which  
 197 uncertainty in the regional head gradient would affect the accuracy of the simulation results, we briefly  
 198 investigate the effect of varying the regional head gradient on the simulated breakthrough curves. In the  
 199 base model, a single constant value of the regional head gradient (0.0014m/m) was used. We repeated  
 200 the numerical simulations with two other regional flow scenarios, namely zero head gradient (0 m/m)  
 201 and a high estimate of the regional head gradient (0.0022 m/m). Unless otherwise mentioned,  
 202 subsequent results and discussions refer to the base model.

203

### 204 **2.3 Tracer and contaminant transport model**

205 Three indicators of effluent spreading are analyzed: Cl:Br, solution EC, and concentrations of the  
 206 antiepileptic pharmaceutical carbamazepine. We also simulate a generic tracer with identical effluent  
 207 concentration timeseries as carbamazepine to illustrate the effect of adsorption and biodegradation on  
 208 solute transport. We assume that Cl:Br (Davis et al., 1998) and EC (Chaali et al., 2013; Scott et al.,  
 209 2020) behave as tracers of the effluent, and carbamazepine as a reactive solute that undergoes  
 210 instantaneous equilibrium adsorption and first-order biodegradation (Durán-Álvarez et al., 2012;  
 211 Williams et al., 2014; Williams et al., 2006). Although adsorption isotherms (e.g. Langmuir isotherm)  
 212 and biodegradation rates (e.g. Michaelis-Menten kinetics) generally follow a non-linear functional  
 213 response with respect to the concentration of the solute being transported, the trace concentrations of  
 214 CECs in the effluent would be small enough for the isotherms and rates to be effectively first-order.

215

216 For all substances except EC, we assume that all solutes in soil water are taken up by crop roots along  
217 with the water regardless of concentration; this is reasonable for CECs, which are present in trace  
218 amounts (Christou et al., 2019). As Cl:Br is a ratio of trace elements, not a concentration, it is  
219 reasonable that root uptake does not affect levels in the soil water. Since root salt uptake rates increase  
220 linearly with soil salinity up to some physiological threshold (Moya et al., 1999), we assume for simplicity  
221 that the maximum root uptake concentration of the ions that contribute to EC is the rainwater  
222 concentration. The rainwater ionic content is small compared to the groundwater and effluent, thus our  
223 implementation is in principle similar but more realistic than other studies in the literature (e.g. Siyal et  
224 al., 2013) that assume no ions are taken up by roots. In the simulations, excess ionic content in the soil  
225 water beyond the rainwater concentration is left behind in the soil water, where it accumulates and  
226 increases the EC.

227

228 The greatest determinant and the largest source of uncertainty regarding solute fate is the adsorption  
229 coefficient and the biodegradation rate, as they span multiple orders of magnitude, are highly uncertain  
230 in the field, and vary not only with CEC identity but also environmental parameters. In this study we  
231 focus on tracers and a relatively mobile and persistent CEC (carbamazepine), and investigate whether  
232 they may contaminate crops and the wider environment. The opposite extreme of immobile CECs  
233 represent a rather trivial case (with respect to a contaminant transport model), where the CECs are  
234 mostly adsorbed or biodegraded within the immediate vicinity of the irrigation pipes (Narain-Ford et al.,  
235 2022). Adsorption coefficients and biodegradation rates of carbamazepine available in the literature vary  
236 over orders of magnitude, depending on environmental factors and in-situ physical and biochemical  
237 conditions (Durán-Álvarez et al., 2012; Williams et al., 2014; Williams et al., 2006). Therefore, we  
238 calibrated these biochemical parameters so that the simulated breakthrough curves match the observed  
239 carbamazepine concentrations in the field. This resulted in a half-life of 125 days (biodegradation rate  
240 coefficient of  $0.008 \text{ day}^{-1}$ ) and an adsorption coefficient of  $1 \text{ L/kg}$ , implying a retardation factor of 2.5,  
241 falling well within the range provided in the literature.

242

243 Daily effluent Cl:Br ratio, EC, and carbamazepine concentrations from the field site were interpolated  
244 from the two to four effluent samples measured per year and used as realistic input values for the model  
245 analysis. Daily effluent EC values became available after June 2018, and were incorporated into the  
246 simulations. The Cl:Br ratio of rainwater is estimated at 100 from samples taken from the shallow soil  
247 (20cm depth) in 2016, and agrees roughly with the literature (e.g. Davis et al, 1998). The EC of  
248 rainwater is estimated at  $100 \mu\text{S/cm}$  from early shallow soil samples, and also agrees in general with the  
249 literature (e.g. Zdeb et al (2018)). Groundwater Cl:Br (300) and EC ( $800 \mu\text{S/cm}$ ) were estimated from  
250 field samples obtained from 4m beneath the soil surface or deeper, as they both are uniformly and  
251 constantly measured at these respective values over the entire subsurface profile deeper than 4m  
252 (Figure 2), during the measurement period. These values are also in approximate agreement with  
253 various studies in the literature on environmental Cl:Br and EC values (e.g. Alcalá and Custodio, 2008;  
254 Van den Brink et al., 2007). Groundwater and rainwater carbamazepine concentrations are assumed to  
255 be zero. Concentration flux boundary conditions were applied for solute transport at all boundaries. Daily  
256 effluent Cl:Br ratio, EC, and carbamazepine concentrations from the field site were interpolated from the  
257 two to four effluent samples measured per year and used as realistic input values for the model analysis.

258

### 259 3. Results

#### 260 3.1 Hydrology

261 Model results show that the system is able to stably maintain the groundwater level within a narrow band  
262 during the crop season. Most of the variations in groundwater levels occur during the drainage season,  
263 because then the drains control the fluxes in only one direction. In other words, during the drainage  
264 season, the drains remove water when the groundwater level is high, but do not add water when the  
265 groundwater level is low, unlike during the crop season. As the maize crops grow throughout the crop  
266 season that spans from May to September, their water requirements increase. Hence, evapotranspiration  
267 rates gradually increased between the start and the end of the crop season. However, the precipitation  
268 volume was low in May and June, and significantly higher in July, August and September, in accordance  
269 with historical averages. Overall, these trends cause the irrigation flux to be at a maximum midway  
270 through the crop season (Figure 4a). Therefore, such a subsurface irrigation system must be designed to  
271 meet the large water demands of July and August.

272

273 The evapotranspiration rates were at a minimum in January, while precipitation rates in January were  
274 around the annual average. Hence, the surplus precipitation (P-ET) is at a maximum in January, which  
275 causes most drainage to occur in January (Figure 4a). Since there is a period of three months between  
276 the end of the crop season and January, most solutes intercepted and recovered by the drains will be  
277 from the outer edge of the plume, which was injected at the start of the crop season and transported to  
278 the root zone by capillary flux during the crop season, and which is moving back into the saturated zone  
279 in January (Figure 5a). Note that lateral advection is minimal above the water table, hence the solutes  
280 migrating downwards at this time from the unsaturated zone to the water table can be intercepted by the  
281 drains. On the other hand, 'newer' solutes that were injected near the end of the crop season would have  
282 left the vicinity of the drains by January through lateral and downwards advection, and either be  
283 discharged into the environment, or extracted by a downstream drain if the plume does not sink too  
284 quickly (Figure 5b). Since the biodegradation of CECs require the solutes to reside in the soil for a period  
285 of time, and since (first-order) biodegradation has diminishing returns with increased residence times, it  
286 is beneficial that 'older' effluent is recovered by drainage instead of 'newer' effluent. The 'older' effluent  
287 that is recovered would comprise a larger fraction of non-biodegradable contaminants that pose a larger  
288 risk of long-term accumulation in the soil, while the 'newer' effluent left in the soil would be able to  
289 biodegrade further. Simulations (not shown) with a non-retarding but biodegradable solute indeed result  
290 in lower drained fractions of solute mass than full tracers.

291

292 Table 2 shows the water balances of the simulations and field experiment. The incoming regional  
293 groundwater flow (Figure 4b), outgoing downwards flux (Figure 4c), and outgoing regional flow (Figure  
294 4d), are positively related to the height of the groundwater level. Of these three boundary fluxes, the  
295 outgoing regional flow is the most sensitive, while the incoming regional flow is the least sensitive to the  
296 groundwater level. The outgoing fluxes vary greatly over time because of irrigation, drainage, and crop  
297 evapotranspiration, which greatly affect the water balances and groundwater levels of the domain. The  
298 downwards flux varies less over time than the outgoing regional flow, which reflects that the resistance  
299 of the bottom boundary (implicit in the deep drainage bottom boundary condition) is larger than that of  
300 the resistance to horizontal flow. Most of the variations in these fluxes occur during the drainage season,  
301 because as previously discussed, most of the fluctuations in groundwater levels occur then. By reducing  
302 the groundwater levels and hence the outwards fluxes of water and solute, drainage outside of the crop  
303 season helps arrest the spreading of effluent.

304

305 Table 2 shows that more irrigation is required and less drainage of water occurs, as the regional flow  
306 head gradient decreases. This occurs because the natural (non-irrigated) average groundwater level  
307 decreases as the regional head gradient decreases. For this same reason, the vertical outflow is smaller  
308 when the regional head gradient is smaller. Altogether, the saturated zone flux out of the simulated  
309 domain (lateral + vertical) is lowest when there is no regional flow, even though the irrigation flux is  
310 higher and drainage flux is lower. This means that the rate of transport of effluent in the saturated zone  
311 increases with the rate of regional flow: the average outwards flux in the high regional flow scenario is  
312 about 1.6 times that of the zero regional flow scenario. The absence of regional flow does not necessarily  
313 imply that no lateral discharge of water from the simulated domain occurs. When hydraulic gradients  
314 arise between the simulated domain and the boundaries due to precipitation or irrigation in excess of  
315 evapotranspiration, not all the excess water will be discharged downwards through the aquifer bed, as  
316 some water will be discharged laterally to the downstream boundary. Therefore, the lateral discharge is  
317 significant even when the regional head gradient is zero.

318

### 319 3.2 Tracer transport

320 The simulated total irrigation and drainage volumes show good agreement with the field observations  
321 (Table 2). The simulated breakthrough curves also show good agreement in general with the field data  
322 (Supplementary material Figure S2.1 – S2.6). In this section (Section 3), key points in the solute mass  
323 balances (Table 3) and breakthrough curves (Supplementary material Figure S2.1 – S2.6) are  
324 elaborated. The fit between simulation data and field measurements appears slightly better for Cl:Br  
325 than for the EC, especially at the measuring points midway between drains. This is consistent with Cl:Br  
326 being likely a more reliable tracer than EC, because Cl:Br is more conservative (Davis et al., 1998) than  
327 EC (Pellerin et al., 2008).

328

329 Results of the base model show that the solute concentrations in the root zone (0.6m depth and above)  
330 reset to nearly background levels before the start of every crop season, with no evidence of long-term  
331 accumulation, due to the large excess precipitation that occurs outside the crop season. This is in  
332 agreement with field observations for a normal hydrological year (Narain-Ford et al., 2022). The tracer  
333 reaches the root zone within the first crop season, and achieves an annual periodic steady-state at the  
334 end of the drainage season in terms of effluent plume shape, location, size, solute concentrations, and  
335 solute mass balances within four years. Therefore, the size of the model domain and a simulation period  
336 of four years is sufficient for long-term analyses of the system.

337

338 During the crop season, the effluent plume moves upwards due to capillary rise when crop water  
339 requirements are not fulfilled by precipitation. Therefore, the upper part of the effluent plume rises in the  
340 summer to above drain level, then sinks back to drain level during the drainage season, and may be  
341 partially drained away. For EC, where we assumed that the maximum root uptake concentration is the  
342 rainwater level, the root zone concentration may significantly exceed the effluent concentration during  
343 the crop season. This is because the ions that contribute to EC are left behind in the soil when water is  
344 absorbed by crops, increasing the EC of the remaining soil water, as was also previously observed by  
345 Siyal et al (2013) and Fujimaki et al (2006). In our simulations, this is observed only in the soil directly  
346 above a drain, and not in the root zone soil midway between drains, because little effluent reaches the  
347 root zone midway between drains. Such large EC levels will decrease to ambient levels by the start of the  
348 following crop season, and thus should not result in long-term salt accumulation. Hence, crop  
349 contamination that might occur during any one irrigation period would likely not carry over to the  
350 following years, regardless of whether they accumulate in the root zone (EC) or not (Cl:Br). However, if  
351 the effluent is very saline, there is a possibility that the irrigation system causes crops directly above  
352 drains to experience salinity stress during dry years (Heidarpour et al., 2007).

353

### 354 **3.3 Reactive solute transport**

355 The mass balances of carbamazepine and the generic tracer are presented in Table 3. No downwards  
356 vertical discharge of carbamazepine from the model domain occurs, due to the effects of adsorption and  
357 biodegradation. For the generic tracer, the amount of downwards vertical solute discharge from the  
358 domain is finite but essentially negligible. Furthermore, less than 10% of the generic tracer and 1% of  
359 carbamazepine are taken up by the crop (Table 3). Hence, the model shows that most of the subirrigated  
360 solutes, whether tracers or carbamazepine, is advected laterally out of the domain along with regional  
361 groundwater flow.

362

363 Small amounts of carbamazepine spread to the sampling points directly above and below drains within  
364 four years. Comparatively much smaller amounts of carbamazepine spread to the soil and aquifer  
365 midway between drains. The mass influx of the generic tracer and carbamazepine at the drains varies  
366 between 0mg to  $10^{-2}$ mg per day during subirrigation. The generic tracer mass flux at the downstream  
367 lateral boundary reaches  $10^{-3}$ mg per day by the first crop season, and remains above that level for most  
368 of the rest of the simulation. However, carbamazepine mass fluxes at the downstream lateral boundary  
369 never exceeds  $10^{-3}$ mg per day, and only reaches  $10^{-4}$ mg per day during the second crop season. No  
370 significant levels of the generic tracer nor carbamazepine reaches the bottom boundary even after four  
371 years. In the phreatic groundwater, carbamazepine spreads less than 3m from the drains after four  
372 years. Hence, the transport of carbamazepine is highly limited compared to that of the tracer.

373

374 When drainage occurs during the crop season, the concentrations of tracer and carbamazepine in the  
375 drained water are similar. When drainage occurs outside the crop season, the concentration of  
376 carbamazepine drained is larger than the tracer, despite carbamazepine undergoing biodegradation,  
377 because adsorption retains the carbamazepine plume close to the drains. This explains why more  
378 carbamazepine than tracer mass is drained in total (Table 3), even though carbamazepine biodegrades in  
379 the soil but not the tracer. This means that immobile contaminants are more likely to be recovered  
380 during drainage than mobile contaminants. Hence, highly immobile and persistent contaminants can  
381 potentially be prevented from accumulating in the agricultural soil by draining it during wet periods, both  
382 during and outside the crop season.

383

384 Differences in the mobility of the tracer and carbamazepine result in different spatial distributions of root  
385 solute uptake. The root zone directly above drains receives the most solutes due to capillary rise. Table 3  
386 shows that the relative amounts of total root solute uptake differ with the horizontal position and depth  
387 of the roots. For the tracer, the roots at the nodes at 0.2m depth take up roughly four times as much  
388 tracer as the roots at 0.6m depth, even though solute concentrations are 10% higher at 0.6m depth,  
389 because the root density is four times larger at 0.2m depth. The roots directly above drains take up  
390 roughly four times as much tracer as the roots midway between drains, because solute concentrations  
391 directly above drains are two to four times larger. These patterns are also observed for carbamazepine.  
392 Carbamazepine uptake directly above drains is over ten times that midway between drains, because  
393 adsorption arrests the spreading of carbamazepine. Therefore, most root uptake of tracer and  
394 carbamazepine occurs directly above drains, and this spatial heterogeneity in root solute uptake is  
395 stronger for less mobile and less persistent solutes.

396

397 Unlike the tracer, for which appreciable levels of root solute uptake, horizontal discharge and vertical  
398 discharge were observed, very little carbamazepine had been taken up by crops or discharged from the  
399 domain by the end of the simulation (Table 3). For carbamazepine too, concentrations in the root zone  
400 essentially reset on an annual basis due to the annual precipitation surplus, which means that the crop  
401 solute uptake of carbamazepine is not expected to increase with the number of years of operation of the  
402 subirrigation system. Since less than 1% of the irrigated carbamazepine is taken up by crops, and since  
403 most crop solute uptake of carbamazepine is concentrated in roots directly above the drains,  
404 carbamazepine levels in crops is likely negligible everywhere except directly above drains, where it is  
405 present in very small concentrations. This also implies that the system studied here might not be suitable  
406 for irrigation in a climate with an annual precipitation shortage.

407

408 Here we highlight the key findings of the experimental data analyses (Narain-Ford et al, 2022) and how  
409 they relate to the results of the model introduced in this study. Of the 55 CECs found in the wastewater  
410 effluent but not in the control field beside the experimental plot, the fraction of CECs classified as mobile  
411 and persistent (MP CECs) is 19/55. Next to the surface water stream located 5m beside the agricultural  
412 plot, and in deep groundwater under the agricultural plot, the average detected concentrations of MP  
413 CECs as a fraction of the effluent concentrations was smaller than 0.01 in deep groundwater and in the  
414 surface water stream on all sampling occasions. An exception was that in the middle of the crop season  
415 during the drought of 2018, somewhat elevated levels of MP CECs were detected next to the surface  
416 water stream, but not in deeper groundwater. Less than 1% of MP CEC mass reaches deeper  
417 groundwater in the field site. In addition, from the field data we observe that the concentrations of all  
418 CECs in the root zone, regardless of mobility or persistence, reset to background levels by the start of  
419 the following year's crop season, except at very close distances from the drains, or if there is a period of  
420 severe drought such as that of 2018. In the field experiment, carbamazepine levels in crop samples  
421 obtained in September 2019 (a hydrologically typical year with no drought) based on solid-phase  
422 extraction of 30g plant material were everywhere below the detection limit (6ng/L), including for crops  
423 directly above drains. All of the above experimental results agree with the introduced model.

424

### 425 **3.4 Effects of regional groundwater fluxes on solute transport**

426 Despite the large effect of the regional head gradient on the breakthrough curves, varying the regional  
427 head gradient had little effect on the relative solute mass balance (Table 3). Most importantly, in the  
428 simulations with high and zero regional head gradients, the main findings of the base model continue to  
429 apply: Crop solute uptake is around 10% for tracers and 1% for carbamazepine and occurs primarily  
430 directly above irrigation drains, little tracer mass seeps to deeper aquifers, no carbamazepine seeps to  
431 deeper aquifers, little solute mass is drained by the drainage system, and the rest of the irrigated solute  
432 mass is discharged horizontally out of the simulated domain, in agreement with field observations  
433 (Narain-Ford et al., 2022). Therefore, uncertainty in the regional head gradient does not undermine the  
434 findings of the study. In fact, we have shown that while the regional head gradient may affect the rate at  
435 which CECs are laterally advected, it does not significantly change our conclusions relating to crop  
436 contamination risk and the overall mass balance of the CECs. Since there is an annual precipitation  
437 surplus, the average annual transport direction of the CECs can only be laterally downstream and/or  
438 vertically downwards, regardless of the regional groundwater head gradient. Since the calibrated lateral  
439 flow resistance is effectively much lower than the downwards flow resistance, the transport of CECs is  
440 primarily lateral even in the absence of regional flow. This explains why the relative solute mass balance  
441 is not sensitive to the regional head gradient.

442

443 When the regional head gradient is low, the natural groundwater level is deeper, therefore requiring a  
444 higher irrigation flux to maintain target water table levels. In the base model (0.0014m/m head  
445 gradient), 16.3mg of carbamazepine was irrigated over the four year simulation period (Table 3). The  
446 corresponding values in the model with no regional flow (0 m/m) and high regional flow (0.0022m/m)  
447 were 25.4mg and 10.9mg respectively, which implies that even such a large uncertainty in regional head  
448 gradient would translate only to a 50% difference in the irrigated solute mass. Nevertheless, in practice  
449 it is easy to monitor the absolute volume of water used by the irrigation system. Therefore, knowledge of  
450 the relative solute mass balance, which is not sensitive to the regional head gradient, is sufficient to  
451 evaluate the fate of the irrigated CECs.

452

## 453 **4 Discussion**

### 454 **4.1 Limitations of the base numerical model**

455 The numerical model is unable to describe the rapid rise in CEC concentrations at two observation points  
456 directly beneath an irrigation pipe. The measurement points located 0.8m and 1.3m beneath drain level,  
457 directly below the drains, are among the deepest measurement points where effluent has been detected  
458 in the field site. For these two measurement points, the base model consistently and significantly  
459 underestimates concentrations of Cl:Br, EC, and carbamazepine (Supplementary material Figure S2.1,  
460 S2.3, S2.5 e and f). The fact that this is observed experimentally for all three modelled compounds,  
461 which have vastly different adsorption, biodegradation, and accumulation behavior in the soil, suggests a  
462 physical rather than chemical reason for the discrepancy. A likely explanation is that in the field  
463 experiment some solutes are rapidly transported vertically downwards from the pipes by preferential flow  
464 due to soil heterogeneity, a mechanism not considered in the model.

465

466 Further evidence that vertical preferential flow is likely the cause of the discrepancy is that measured  
467 concentrations of carbamazepine at these outlier points are almost identical to measured effluent  
468 concentrations, which implies that carbamazepine did not experience significant adsorption and  
469 biodegradation while it was transported from the irrigation drains to those points, despite exhibiting  
470 retardation across the rest of the domain. The fast downwards transport of solutes described above is  
471 consistent with solute transport in large macropores or fractures, which have small pore surface-area-to-  
472 volume ratios and hence less adsorption sites, thereby causing effluent to travel vertically downwards  
473 much faster than simulated in the model.

474

475 In general, the simulations with no regional head gradient result in breakthrough curves that deviate  
476 more significantly from field data than the base model, especially at observation points between drains.  
477 However, at the two aforementioned observation points where the base model tends to fit poorly with  
478 the experimental data (directly beneath drains, 0.8m and 1.3m below drain level), the simulations with  
479 no regional head gradient have better fits with the experimental data than the base model. Since the  
480 base model has better fits with the data when considering all other observation points, it is unlikely that  
481 overestimation of the regional head gradient is responsible for the base model's poor fitting at 0.8m and  
482 1.3m directly beneath drains. The fact that the zero head gradient case exaggerates the extent of  
483 downwards transport of solutes also reinforces the hypothesis that vertical preferential flow is the cause  
484 of the rapid increase in effluent concentrations 0.8m and 1.3m directly beneath drains in the field.

485

486 In this section we have argued that the disagreement between model and field data at these two points  
487 is very likely caused by vertical preferential flow. Since the disagreement occurs only for two observation  
488 points out of twelve, and since these two points are located at the same direction from the drains  
489 suggesting a common unknown cause, we conclude that the model approximates the field situation well  
490 in general. Hence, the model successfully captures the general but simplified flow and solute transport  
491 patterns observed in the field. This also implies that although most solutes are laterally advected out of  
492 the subsurface of the agricultural field, the presence of vertical preferential flow may lead to some  
493 downwards leaching, although this adverse possibility was not observed in the experiment (Figure 2)

494

**4.2 Effects of soil heterogeneity on solute fate**

Section 4.1 shows that soil heterogeneity may cause solutes to be transported within the soil more rapidly and at higher concentrations. Furthermore, possible clogging of the soil around irrigation drains due to the growth of biofilms, precipitation of minerals, and deposition of particulate matter was observed in the experiment. This may eventually alter the hydrological and biogeochemical properties of the soil, in a spatially heterogeneous manner. Therefore, we further investigate the effects of soil heterogeneity on solute fate, using a simple model of soil heterogeneity. To the generic tracer base model, we add soil heterogeneity with Miller-Miller similitude (Miller and Miller, 1956), where the pressure head and hydraulic conductivity at a certain soil water content are scaled according to a scaling factor  $m$ , which is randomly distributed across space in the soil (see Roth (1995) for more information). Roth (1995) found that the spatial structures of soil hydraulic properties (water retention, pressure head, and flow velocity) becomes highly sensitive to random heterogeneity in the scaling factor  $m$  if the standard deviation of  $\log_{10}(m)$ ,  $\sigma_m$ , is larger than 0.7. Therefore, we simulate the generic tracer base model with 30 random fields of the scaling factor  $m$ , with horizontal and vertical exponential autocorrelation lengths of 2m and 0.5m respectively, and with  $\sigma_m = 0.25$  and  $\sigma_m = 0.75$ , to simulate weak and strong heterogeneity respectively.

511

Summary statistics boxplots of the simulations with weak heterogeneity (Figure 6a) show that the medians and means of the outcomes are very close to the homogeneous base model. The simulated heterogeneity is responsible for less than a half-order of magnitude variation in outcomes. Consider that the 30 random fields simulated can be considered as 30 subplots of a single larger agricultural plot. The statistical outcomes therefore imply that in an agricultural plot with weakly heterogeneous soils, crop solute uptake and saturated zone solute discharge should be spatially heterogeneous but on average be similar to that of a homogeneous soil. However, spatially uneven distribution of crop solute uptake is already a feature of the subsurface irrigation system even in homogeneous soils (Section 3.3), as most crop solute uptake occurs directly above the individual drains, whereas crops located midway between drains take up little solute.

522

Strong heterogeneity, on the other hand, led to significantly worse environmental outcomes compared to the base model (Figure 6b). On average, about twice as much effluent had to be irrigated into the system to maintain the target groundwater levels. More saturated zone solute discharge occurred, while less solute was drained away. Therefore, most of the additional irrigated effluent caused by soil heterogeneity is discharged into the saturated zone through high conductivity channels. Consequently, solutes and CECs in the saturated zone has a farther reach and larger mass, which may render subirrigation unfeasible in strongly heterogeneous soils. However, the root solute uptake was on average similar as in homogeneous soils, because the crop solute uptake is limited by the water requirements of the crop. It is also noteworthy that of all the key simulation outcomes, root solute uptake had the lowest variance across realizations, for both mild and strong heterogeneity. Therefore, even though spatial heterogeneity was present both in the root zone and beneath the root zone, most of its effects were concentrated in the saturated zone.

535

Altogether, this analysis shows that crop contamination is on average similar in homogeneous and heterogeneous soils, even under strong heterogeneity. In contrast, as we have shown, groundwater contamination in the saturated zone is more sensitive to soil heterogeneity. This is consistent with our observation in Section 4.1 that field sampled solute concentrations in the saturated zone displayed more behavior that was not explained by the homogeneous model, than sampled concentrations in the unsaturated zone.

542

Although weak soil heterogeneity had little impact on solute mass balance on average, it had a large effect on solute breakthrough curves at observation points, due to the possibility of streamlines bypassing or concentrating around observation points. Even under weak heterogeneity, peak tracer concentrations at observation points (both in the saturated zone and root zone) varied by over a factor of 10 across the individual realizations of heterogeneous simulations (not shown). This agrees with heterogeneity being an explanation for the discrepancies observed in Section 4.1.

549

550 Whether subirrigation with treated wastewater in strongly heterogeneous soils poses a significant  
 551 environmental problem, depends on the ability of contaminants to undergo further in-situ bioremediation  
 552 in the groundwater, and whether the groundwater will be abstracted at downstream locations for other  
 553 uses. Nevertheless, Figure 6b shows that in the strong heterogeneity scenario, AbsContIn,  
 554 AbsContOutRight, and log10AbsContOutDown (see Figure 6 caption for variable name explanations), all  
 555 approximately double. Therefore, these outcomes all appear to be proportionally related. Indeed, across  
 556 the 30 simulations with strong heterogeneity, AbsContIn and AbsContOutRight were related with an R-  
 557 squared of 0.99. Similarly, AbsContIn and log10AbsContOutDown were related by an R-squared of 0.46.  
 558 Hence, even in strongly heterogeneous soils, it is possible to limit lateral contaminant discharge to the  
 559 groundwater by simply lowering the irrigation flux, though water availability for crops may also decrease  
 560 accordingly. Future studies could investigate the effects of soil heterogeneity on geochemically reactive  
 561 CECs. In physically heterogeneous soils, the spatial distribution of adsorption sites and microbes  
 562 responsible for biodegradation will also be heterogeneous, leading to a highly complex problem that is  
 563 beyond the scope of this paper. The potential for short or long term soil structure changes due to  
 564 biomass growth and clogging, and methods to prevent or remediate them, should also be investigated in  
 565 future studies.

566

### 567 **4.3 Environmental impact beyond the agricultural plot**

568 We have shown that most of the effluent leaves the crop field by lateral advection. In heterogeneous  
 569 soils, where more water has to be irrigated to maintain target groundwater levels, most of the additional  
 570 solute mass introduced into the subsurface leaves the plot through lateral advection. Beyond the  
 571 agricultural field, the downwards transport rate of the CECs would decrease further, as the absence of  
 572 irrigation reduces the downwards water fluxes. Therefore, most of the CECs that leave the crop field  
 573 likely remain in the phreatic zone until they are discharged into a surface water body, such as a stream  
 574 or river.

575

576 In Ternes et al's (2007) study of 54 CECs present in treated domestic wastewater in Germany,  
 577 carbamazepine was found to be one of the most persistent and mobile CECs in the soil and phreatic  
 578 zone. Therefore, the spreading of many other CECs in the environment is likely to be even more limited  
 579 than what we have observed for carbamazepine. Any CEC that is more mobile and persistent than  
 580 carbamazepine would exhibit behavior that is intermediate between carbamazepine and tracers, both of  
 581 which have been discussed in this study. Since the effluent would have likely been directly discharged  
 582 into surface water in the absence of the subirrigation system, the subirrigation system therefore possibly  
 583 reduces the adverse environmental impacts associated with treated wastewater discharge, thereby  
 584 leading to better surface water quality in the vicinity of the treatment plant. Still, some attention should  
 585 be paid to possible ecotoxic effects of transformation products (Reemtsma et al., 2016).

586

### 587 **4.4 Potential for further adoption**

588 Around 35% of agricultural land in the Netherlands (NL) is currently drained using subsurface drainage  
 589 pipes. In agricultural land, drainage pipes are mostly 0.9m to 1.2m deep, but can vary slightly depending  
 590 on factors such as soil type, or due to processes such as soil settling (Maasop & Schuiling, 2016). The  
 591 placement of the drains (depth and inter-drain distance) beneath agricultural lands is designed according  
 592 to national standards in which the local soil type and topography are factored (Cultuurtechnische  
 593 Vereniging, 1988). Since the drainage response of the drainage systems are nationally similar, the  
 594 wetting patterns in the soil when subirrigation is performed with similar fluxes should not be too  
 595 different. Under similar hydrological and hydrogeological conditions, this leaves the crop type as likely  
 596 the key determining factor in crop contamination risk, through several aspects of crop physiology that  
 597 could be studied in further detail in future research: the spatial distribution of its roots, its disposition  
 598 towards solute uptake, and its water requirements.

599

600 Drought is another factor that should be considered in the adoption of the proposed subsurface irrigation  
 601 approach with treated wastewater. Our study area in the Netherlands is vulnerable to occasional drought,  
 602 which occurred in 2018–2019 during our study period. In our model, of the total tracer (and  
 603 carbamazepine) solute mass taken up by crops over the four year simulation period (Table 3), 21%  
 604 (21%) occurred in 2016-2017, 35% (43%) occurred in 2018, and 44% (36%) occurred in 2019.  
 605 Simulated crop solute uptake in 2019 was similarly high as in 2018 because some of the solutes irrigated

606 in 2018 remained in the topsoil even by the start of the crop season in 2019, whereas they would have  
607 been flushed away by precipitation in a normal hydrological year. Therefore, soil water concentrations of  
608 contaminants should be monitored more closely during the occasional drought year, and the following  
609 year. If such precautions are taken, then crop contamination risks are manageable in regions that  
610 experience occasional drought. In regions with perpetual drought, the proposed subsurface irrigation  
611 approach is not recommended altogether, as large amounts of water (and CECs) will have to be  
612 introduced into the subsurface, and there is insufficient precipitation to flush out CECs from the root zone  
613 during the non-crop season, possibly leading to accumulation of persistent CECs in the root zone. A  
614 relative precipitation shortage caused by farming crops with large water requirements, instead of by  
615 drought, may pose similar risks. In this regard, note that this study was conducted on maize agriculture,  
616 which is one of the most water-intensive common crops in the Netherlands, aside from tree fruits (LAGO,  
617 1984).

618

619 A new EU regulatory framework intends to stimulate and regulate direct reuse of treated domestic  
620 wastewater for irrigation purposes (European Commission, 2020). A risk management plan (Maffetone &  
621 Gawlik, 2022) and irrigation water quality requirements (Alcade Sanz & Gawlik, 2017) is part of the EU  
622 regulation and includes an analysis of the effect of water reuse on farmers, soil, groundwater and  
623 ecosystems. As water reuse through subirrigation is a special form of irrigation, process-based  
624 knowledge and modeling tools as presented in this study are required to identify potential risks and take  
625 appropriate precaution measures.

626

## 627 **5 Conclusion and outlook**

628 The results and analyses of the model have provided additional understanding of the physical processes  
629 of CEC transport under subsurface irrigation using marginal water in phreatic aquifers, a novel method of  
630 managed aquifer recharge in regions with annual precipitation surpluses. In the long term, effluent  
631 contamination in both the root zone and the phreatic zone within the agricultural plot becomes  
632 periodically steady-state, with larger concentrations during the crop season and nearly background  
633 concentrations during the drainage season. No long-term accumulation of CECs in the root zone occurs  
634 due to the annual precipitation surplus. Despite the possibility of minor crop contamination by mobile  
635 contaminants, most of the crop solute uptake occurred for crops located directly above drains, whereas  
636 crops located midway between drains are barely exposed even to tracers. Combined application with  
637 intercropping, where non-food crops are placed above drains, could be the next step in the development  
638 and adaptation of subsurface irrigation with treated wastewater. Transport of contaminants from the  
639 phreatic zone to deeper groundwater accounts for a negligible portion of the solute mass balance for the  
640 simulated scenarios. Around 90% of the effluent tracer leaves the simulated domain along with lateral  
641 advection by regional groundwater flow, so most tracers in the effluent would end up discharged to  
642 surface water.

643

644 Using the treated wastewater in subsurface irrigation therefore likely leads to better surface water  
645 quality, compared to the alternative of direct discharge of the treated wastewater into rivers and canals.  
646 Furthermore, such a system of subsurface irrigation with treated wastewater may be implemented using  
647 existing subsurface drainage pipes. Using such alternative water resources for agricultural water supply  
648 reduces the use of groundwater resources and other sources of freshwater, which are increasingly under  
649 pressure (Pronk et al., 2021). Hence, this system has the potential to reduce anthropogenic  
650 environmental damage associated with discharge of sewage treatment plant effluent at a low technical  
651 difficulty and initial investment cost.

652

653 Despite the front-loaded initial investment costs, the reduction in groundwater usage, improvements in  
654 the quality of the surface water, and increased crop yields due to improved crop access to water, may  
655 lead to economic returns and wider adoption in the long term. However, this should not lead to a  
656 reduced effort to minimize the contaminant load of wastewater discharged into the environment, as the  
657 capacity of the soil and soil microbes to biodegrade CECs remains uncertain and difficult to quantify  
658 exactly. New EU rules on treating urban wastewater will lead to improved quality of treated wastewater,  
659 thus further reducing the potential environmental impact of using it for irrigation. Of all possible adverse  
660 solute fates, the most sensitive to CEC mobility is crop contamination, as the CEC must rise to the root  
661 zone within a single crop season for this to occur. This did not occur in this study even with tracers,  
662 implying that mobility causes less of an environmental contamination risk than persistence. We therefore

663 recommend that future improvements to water treatment technologies focus on removing contaminants  
664 that persist in the soil, to prevent their proliferation in the wider environment. Immobile but persistent  
665 CECs spread less easily and will be removed from the soil to a larger degree during drainage, whereas  
666 less persistent CECs will more likely be remediated within the soil. Focusing on persistent contaminants  
667 during primary treatment would thus maximize the degree of complementarity between wastewater  
668 treatment technology and nature-based secondary treatment solutions such as the irrigation and  
669 drainage system introduced in this paper.

670

671 The models in this study were constructed loosely within the context of an experimental field in the  
672 Netherlands, and are meant to apply to similar subsurface irrigation and drainage systems in general. A  
673 sensitivity analysis of the model will reveal the environmental and crop safety consequences of adapting  
674 the system to other regions with various hydrogeological and climatic properties. Another avenue for  
675 further research may be to investigate the ecotoxicology and spreading of biodegradation metabolites,  
676 which may not be present in the original CEC cocktail.

677

### 678 **Acknowledgements**

679 This work is part of the research program "Re-Use of Treated effluent for agriculture (RUST)" with  
680 project number ALWGK.2016.016, which is financed by the Netherlands Organization for Scientific  
681 Research (NWO), KWR Water Research Institute (through the program Water in the Circular Economy of  
682 the joint research of the Dutch drinking water companies and De Watergroep), and KnowH2O.

683 **References**

- 684 Alcalde Sanz, L. and Gawlik, B., Minimum quality requirements for water reuse in agricultural irrigation  
685 and aquifer recharge - Towards a water reuse regulatory instrument at EU level Réédition, EUR 28962  
686 EN, Publications Office of the European Union, Luxembourg, 2017, ISBN 978-92-79-77176-7 (print),978-  
687 92-79-77175-0 (pdf), doi:10.2760/804116 (online),10.2760/887727 (print), JRC109291.
- 688 Alcalá, F. J., & Custodio, E. (2008). Using the Cl/Br ratio as a tracer to identify the origin of salinity in  
689 aquifers in Spain and Portugal. *Journal of Hydrology*, 359(1-2), 189-207.
- 690 Beard, J. E., Bierkens, M. F., & Bartholomeus, R. P. (2019). Following the water: Characterising de facto  
691 wastewater reuse in agriculture in the Netherlands. *Sustainability*, 11(21), 5936.
- 692 Bekele, E., Toze, S., Patterson, B., & Higginson, S. (2011). Managed aquifer recharge of treated  
693 wastewater: Water quality changes resulting from infiltration through the vadose zone. *Water Research*,  
694 45(17), 5764-5772.
- 695 Bern, C. R., Breit, G. N., Healy, R. W., Zupancic, J. W., & Hammack, R. (2013). Deep subsurface drip  
696 irrigation using coal-bed sodic water: Part I. Water and solute movement. *Agricultural water  
697 management*, 118, 122-134.
- 698 Bonaiti, G., & Borin, M. (2010). Efficiency of controlled drainage and subirrigation in reducing nitrogen  
699 losses from agricultural fields. *Agricultural Water Management*, 98(2), 343-352.
- 700 Borin, M., Bonaiti, G., & Giardini, L. (2001). Controlled drainage and wetlands to reduce agricultural  
701 pollution: a lysimetric study. *Journal of environmental quality*, 30(4), 1330-1340.
- 702 Borin, M., Bonaiti, G., & Giardini, L. (1998). First result on controlled drainage to reduce nitrate losses  
703 from agricultural sites. In *Water and the environment: innovation issues in irrigation and drainage* (pp.  
704 35-42). E & FN Spon London.
- 705 Cai, Y., Zhao, X., Wu, P., Zhang, L., Zhu, D., & Chen, J. (2019). Effect of soil texture on water  
706 movement of porous ceramic emitters: A simulation study. *Water*, 11(1), 22.
- 707 Chaali, N., Comegna, A., Dragonetti, G., Todorovic, M., Albrizio, R., Hijazeen, D., ... & Coppola, A.  
708 (2013). Monitoring and modeling root-uptake salinity reduction factors of a tomato crop under non-  
709 uniform soil salinity distribution. *Procedia Environmental Sciences*, 19, 643-653.
- 710 Christou, A., Papadavid, G., Dalias, P., Fotopoulos, V., Michael, C., Bayona, J. M., ... & Fatta-Kassinou, D.  
711 (2019). Ranking of crop plants according to their potential to uptake and accumulate contaminants of  
712 emerging concern. *Environmental research*, 170, 422-432.
- 713 Cultuurtechnische Vereniging (1988) *Cultuur technisch vademecum*. Cultuurtechnische Vereniging.  
714 Utrecht, The Netherlands: Rijkskantorengedebouw Westraven
- 715 Davis, S. N., Whittemore, D. O., & Fabryka-Martin, J. (1998). Uses of chloride/bromide ratios in studies  
716 of potable water. *Groundwater*, 36(2), 338-350.
- 717 Devaux, I., Gerbaud, L., Planchon, C., Bontoux, J., & Glanddier, P. Y. (2001). Infectious risk associated  
718 with wastewater reuse: an epidemiological approach applied to the case of Clermont-Ferrand, France.  
719 *Water Science and Technology*, 43(12), 53-60.
- 720 De Wit, J. J., Ritsema, C. J., van Dam, J. C., van den Eertwegh, G., & Bartholomeus, R. (2022).  
721 Development of subsurface drainage systems: Discharge-retention-recharge. *Agricultural Water  
722 Management*, 269, 107677.
- 723 Dingemans, M. M., Smeets, P. W., Medema, G., Frijns, J., Raat, K. J., van Wezel, A. P., & Bartholomeus,  
724 R. P. (2020). Responsible Water Reuse Needs an Interdisciplinary Approach to Balance Risks and  
725 Benefits. *Water*, 12(5), 1264.
- 726 Dole, J. M., Cole, J. C., & von Broembsen, S. L. (1994). Growth of poinsettias, nutrient leaching, and  
727 water-use efficiency respond to irrigation methods. *HortScience*, 29(8), 858-864.

- 728 Durán-Álvarez, J. C., Prado-Pano, B., & Jiménez-Cisneros, B. (2012). Sorption and desorption of  
729 carbamazepine, naproxen and triclosan in a soil irrigated with raw wastewater: Estimation of the sorption  
730 parameters by considering the initial mass of the compounds in the soil. *Chemosphere*, 88(1), 84-90.
- 731 Elliott, J., Deryng, D., Müller, C., Frieler, K., Konzmann, M., Gerten, D., ... & Wisser, D. (2014).  
732 Constraints and potentials of future irrigation water availability on agricultural production under climate  
733 change. *Proceedings of the National Academy of Sciences*, 111(9), 3239-3244.
- 734 Ernst, L. F., & Feddes, R. A. (1979). Invloed van grondwateronttrekking voor beregening en drinkwater  
735 op de grondwaterstand (No. 1116). ICW.
- 736 European Commission (2020) Regulation (EU) 2020/741 of the European Parliament and of the Council  
737 of 25 May 2020 on Minimum Requirements for Water Reuse. *Official Journal of the European Union L*  
738 177/32: pp. 32–55.
- 739 Feddes, R.A., Kowalik, P.J., and Zaradny, H. 1978. Simulation of field water use and crop yield. John  
740 Wiley & Sons, New York.
- 741 Fujimaki, H., Shimano, T., Inoue, M., & Nakane, K. (2006). Effect of a salt crust on evaporation from a  
742 bare saline soil. *Vadose Zone Journal*, 5(4), 1246-1256.
- 743 Gelhar, L. W., & Collins, M. A. (1971). General analysis of longitudinal dispersion in nonuniform flow.  
744 *Water Resources Research*, 7(6), 1511-1521.
- 745 Greskowiak, J., Hamann, E., Burke, V., & Massmann, G. (2017). The uncertainty of biodegradation rate  
746 constants of emerging organic compounds in soil and groundwater—A compilation of literature values for  
747 82 substances. *Water research*, 126, 122-133.
- 748 Haberle, J., & Svoboda, P. (2015). Calculation of available water supply in crop root zone and the water  
749 balance of crops. *Contributions to Geophysics and Geodesy*, 45(4), 285-298.
- 750 Heidarpour, M., Mostafazadeh-Fard, B., Koupai, J. A., & Malekian, R. (2007). The effects of treated  
751 wastewater on soil chemical properties using subsurface and surface irrigation methods. *Agricultural*  
752 *Water Management*, 90(1-2), 87-94.
- 753 Heinen, M., Bakker, G., & Wösten, J. H. M. (2020). Waterretentie-en doorlatendheidskarakteristieken van  
754 boven-en ondergronden in Nederland: de Staringreeks: Update 2018 (No. 2978). Wageningen  
755 Environmental Research.
- 756 Hopmans, J. W., & Stricker, J. N. M. (1989). Stochastic analysis of soil water regime in a watershed.  
757 *Journal of Hydrology*, 105(1-2), 57-84.
- 758 Kacimov, A. R., & Obnosov, Y. V. (2021). Infiltration-induced phreatic surface flow to periodic drains:  
759 Vedernikov–Engelund–Vasil’ev’s legacy revisited. *Applied Mathematical Modelling*, 91, 989-1003.
- 760 LAGO (Werkgroep Landbouwkundige Aspecten), 1984. Landbouwkundige aspecten van  
761 grondwateronttrekking. CoGroWa, Utrecht, 154 pp.
- 762 Liu, Y., Ao, C., Zeng, W., Srivastava, A. K., Gaiser, T., Wu, J., & Huang, J. (2021). Simulating water and  
763 salt transport in subsurface pipe drainage systems with HYDRUS-2D. *Journal of Hydrology*, 592, 125823.
- 764 Lubello, C., Gori, R., Nicese, F. P., & Ferrini, F. (2004). Municipal-treated wastewater reuse for plant  
765 nurseries irrigation. *Water research*, 38(12), 2939-2947.
- 766 Maffettone, R. and Gawlik, B., Technical guidance - water reuse risk management for agricultural  
767 irrigation schemes in Europe, EUR 31316 EN, Publications Office of the European Union, Luxembourg,  
768 2022, ISBN 978-92-76-59112-2, doi:10.2760/590804, JRC129596.
- 769 Massop, H. T. L., & Schuiling, C. (2016). Buisdrainagekaart 2015: update landelijke buisdrainagekaart op  
770 basis van de landbouwmetellingen van 2012 (No. 2700). Alterra, Wageningen-UR.
- 771 Mohammad, M. J., & Mazahreh, N. (2003). Changes in soil fertility parameters in response to irrigation of  
772 forage crops with secondary treated wastewater. *Communications in soil science and plant analysis*,  
773 34(9-10), 1281-1294.

- 774 Moriasi, D. N., Arnold, J. G., Van Liew, M. W., Bingner, R. L., Harmel, R. D., & Veith, T. L. (2007). Model  
775 evaluation guidelines for systematic quantification of accuracy in watershed simulations. *Transactions of*  
776 *the ASABE*, 50(3), 885-900.
- 777 Moya, J. L., Primo-Millo, E., & Talón, M. (1999). Morphological factors determining salt tolerance in citrus  
778 seedlings: the shoot to root ratio modulates passive root uptake of chloride ions and their accumulation  
779 in leaves. *Plant, Cell & Environment*, 22(11), 1425-1433.
- 780 Narain-Ford, D. M., Bartholomeus, R. P., Dekker, S. C., & van Wezel, A. P. (2020). Natural purification  
781 through soils: Risks and opportunities of sewage effluent reuse in sub-surface irrigation. *Rev. Environ.*  
782 *Contam. Toxicol.* 250, 85–117. [https://doi.org/10.1007/398\\_2020\\_49](https://doi.org/10.1007/398_2020_49)
- 783 Narain-Ford, D.M., Bartholomeus, R.P., Raterman, B., van Zaanen, I., ter Laak, T.T., van Wezel, A.P.,  
784 Dekker, S.C., 2021. Shifting the imbalance: Intentional reuse of Dutch sewage effluent in sub-surface  
785 irrigation. *Sci. Total Environ.* 752, 142214. <https://doi.org/10.1016/j.scitotenv.2020.142214>
- 786 Narain-Ford, D. M., van Wezel, A. P., Helmus, R., Dekker, S. C., & Bartholomeus, R. P. (2022). Soil self-  
787 cleaning capacity: Removal of organic compounds during sub-surface irrigation with sewage effluent.  
788 *Water Research*, 119303.
- 789 Nham, H. T. T., Greskowiak, J., Nödler, K., Rahman, M. A., Spachos, T., Rusteberg, B., ... & Licha, T.  
790 (2015). Modeling the transport behavior of 16 emerging organic contaminants during soil aquifer  
791 treatment. *Science of the Total Environment*, 514, 450-458.
- 792 Pellerin, B. A., Wollheim, W. M., Feng, X., & Vörösmarty, C. J. (2008). The application of electrical  
793 conductivity as a tracer for hydrograph separation in urban catchments. *Hydrological Processes: An*  
794 *International Journal*, 22(12), 1810-1818.
- 795 Peng, S., He, Y., Yang, S., & Xu, J. (2015). Effect of controlled irrigation and drainage on nitrogen  
796 leaching losses from paddy fields. *Paddy and water environment*, 13(4), 303-312.
- 797 Pronk, G., Stofberg, S., Van Dooren, T., Dingemans, M., Frijns, J., Koeman-Stein, N., Smeets, P.,  
798 Bartholomeus, R., 2021. Increasing Water System Robustness in the Netherlands: Potential of Cross-  
799 Sectoral Water Reuse. *Water Resources Management: 1-15*.
- 800 Qadir, M., Wichelns, D., Raschid-Sally, L., McCornick, P. G., Drechsel, P., Bahri, A., & Minhas, P. S.  
801 (2010). The challenges of wastewater irrigation in developing countries. *Agricultural water management*,  
802 97(4), 561-568.
- 803 Rauch-Williams, T., Hoppe-Jones, C., & Drewes, J. E. (2010). The role of organic matter in the removal  
804 of emerging trace organic chemicals during managed aquifer recharge. *Water research*, 44(2), 449-460.
- 805 Reemtsma, T., Berger, U., Arp, H. P. H., Gallard, H., Knepper, T. P., Neumann, M., ... & Voogt, P. D.  
806 (2016). Mind the Gap: Persistent and Mobile Organic Compounds Water Contaminants That Slip  
807 Through.
- 808 Richardson, S. D., & Ternes, T. A. (2018). Water analysis: emerging contaminants and current issues.  
809 *Analytical chemistry*, 90(1), 398-428.
- 810 Roth, K. (1995). Steady state flow in an unsaturated, two-dimensional, macroscopically homogeneous,  
811 Miller-similar medium. *Water Resources Research*, 31(9), 2127-2140.
- 812 Saefuddin, R., Saito, H., & Šimůnek, J. (2019). Experimental and numerical evaluation of a ring-shaped  
813 emitter for subsurface irrigation. *Agricultural water management*, 211, 111-122.
- 814 Scott, I. S., Huang, C. H., & Bowling, L. C. (2020). The use of electrical conductivity to develop  
815 temporally precise breakthrough curves in tracer injection experiments. *Journal of Hydrology*, 588,  
816 124998.
- 817 Šimůnek, J., & Hopmans, J. W. (2009). Modeling compensated root water and nutrient uptake. *Ecological*  
818 *modelling*, 220(4), 505-521.
- 819 Šimůnek, J., Van Genuchten, M. T., & Šejna, M. (2016). Recent developments and applications of the  
820 HYDRUS computer software packages. *Vadose Zone Journal*, 15(7).

- 821 Siyal, A. A., Van Genuchten, M. T., & Skaggs, T. H. (2013). Solute transport in a loamy soil under  
822 subsurface porous clay pipe irrigation. *Agricultural Water Management*, 121, 73-80.
- 823 Ternes, T. A., Bonerz, M., Herrmann, N., Teiser, B., & Andersen, H. R. (2007). Irrigation of treated  
824 wastewater in Braunschweig, Germany: an option to remove pharmaceuticals and musk fragrances.  
825 *Chemosphere*, 66(5), 894-904.
- 826 Van Den Brink, C., Frapporti, G., Griffioen, J., & Zaadnoordijk, W. J. (2007). Statistical analysis of  
827 anthropogenic versus geochemical-controlled differences in groundwater composition in The Netherlands.  
828 *Journal of Hydrology*, 336(3-4), 470-480.
- 829 Wesseling, J. G., J. A. Elbers, P. Kabat, and B. J. van den Broek, SWATRE: instructions for input, Internal  
830 Note, Winand Staring Centre, Wageningen, the Netherlands, 1991.
- 831 Williams, C. F., Watson, J. E., & Nelson, S. D. (2014). Comparison of equilibrium and non-equilibrium  
832 distribution coefficients for the human drug carbamazepine in soil. *Chemosphere*, 95, 166-173.
- 833 Williams, C. F., Williams, C. F., & Adamsen, F. J. (2006). Sorption-desorption of carbamazepine from  
834 irrigated soils. *Journal of environmental quality*, 35(5), 1779-1783.
- 835 Yang, Y., Ok, Y. S., Kim, K. H., Kwon, E. E., & Tsang, Y. F. (2017). Occurrences and removal of  
836 pharmaceuticals and personal care products (PPCPs) in drinking water and water/sewage treatment  
837 plants: A review. *Science of the Total Environment*, 596, 303-320.
- 838 Zdeb, M., Papciak, D., & Zamorska, J. (2018). An assessment of the quality and use of rainwater as the  
839 basis for sustainable water management in suburban areas. In *E3S Web of conferences* (Vol. 45, p.  
840 00111). EDP Sciences.
- 841

842 Table 1: Parameters used in the simulations. Soil 1 is present from field level to 0.2m depth. Soil 2 is  
 843 present from 0.2m to 0.6m depth. Soil 3 makes up the bulk of the aquifer. Sources of parameter values:  
 844 1) Heinen et al (2020); 2) Dutch geological survey (TNO); 3) Ernst and Feddes (1979); 4) Calibrated to  
 845 experimental data; 5) Estimates

Parameter	Value	Source
$\theta_r$ (soil 1,2,3) Residual saturation	0.01	1
$\theta_s$ (soil 1,2,3) Maximum saturation	0.42	1
$\alpha$ (soil 1,2,3) [1/m] van Genuchten soil water retention parameter	2	1
$n$ (soil 1,2,3) van Genuchten soil water retention parameter	1.5	1
$K_s$ (soil 1) [m/day] Saturated conductivity	0.5	1
$K_s$ (soil 2) [m/day] Saturated conductivity	2	1
$K_s$ (soil 3) [m/day] Saturated conductivity	5	1
$L$ (all soils) Tortuosity parameter	0.5	1
Regional head gradient	0.0014	2
Reference depth $Z$ [m] Deep drainage boundary parameter	0	3
$A$ [m/day] Deep drainage boundary parameter	0.0025	3

$B$ [1/m] Deep drainage boundary parameter	-1.250	3
Water table depth at downstream boundary [m]	1.6	4
Conductivity of downstream boundary [m/day]	0.02	4
Irrigation drain conductivity [m/day]	0.025	4
Irrigation pressure [m]	0.3	4
Drainage backpressure [m]	0.3	4
Longitudinal dispersivity $D_l$ [m]	0.2	5
Transverse dispersivity $D_t$ [m]	0.02	5
Soil bulk density $\rho$ [kg/L]	1.5	5

846

847

848

849 Table 2: Water mass balances over the entire duration of the modelled scenarios. Water balances are  
 850 expressed in millimeters for comparison with rainfall volumes. Field data for entries with a dash were not  
 851 measured.

852

<b>Water balances</b>	<b>Irrigated water (mm)</b>	<b>Drained water (mm)</b>	<b>Crop water uptake (mm)</b>	<b>Rainfall (mm)</b>	<b>Lateral flow in (mm)</b>	<b>Lateral flow out (mm)</b>	<b>Vertical flow out (mm)</b>
Field data	1828	280	-	-	-	-	-
Base model	1895	269	1916	3152	2785	4041	1004
No regional flow model	2997	39	1916	3152	0	2870	831
High regional flow model	1218	728	1916	3152	4339	4722	1127

853

854

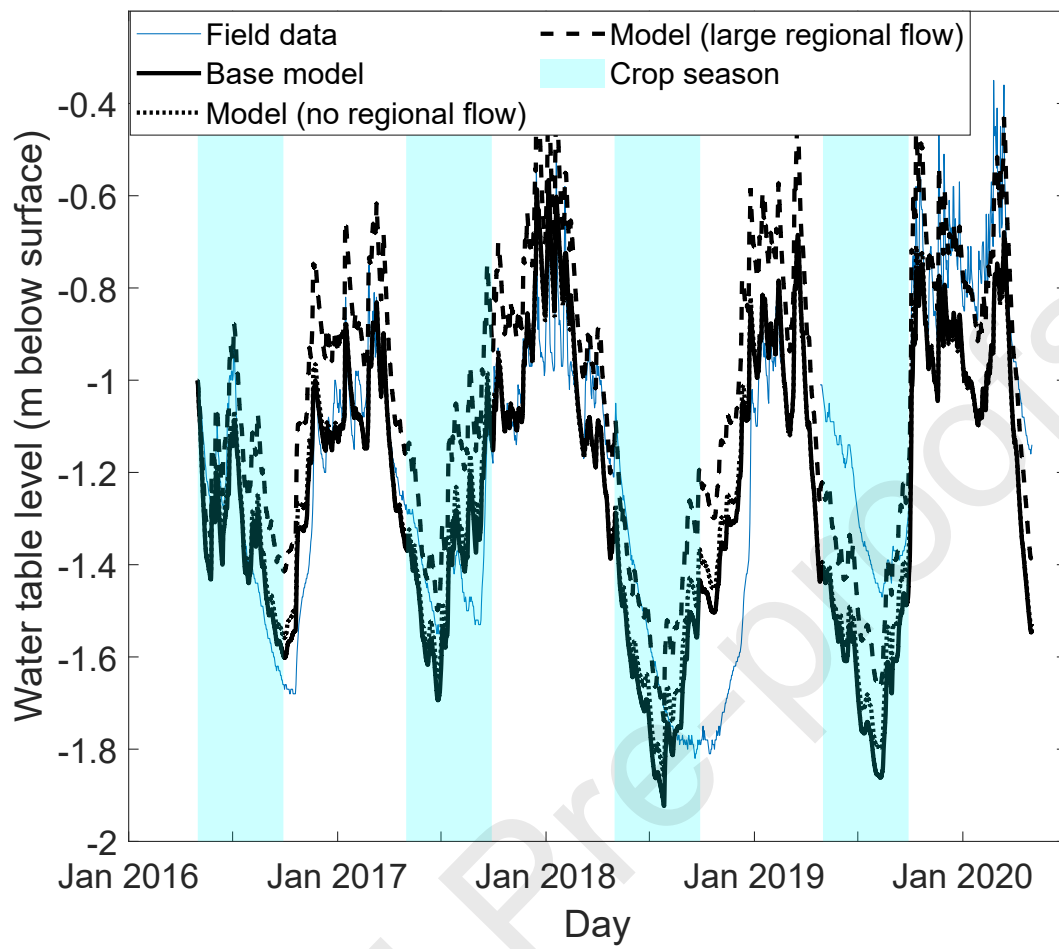
855 Table 3: Solute mass balances over the entire duration of the modelled scenarios. Since each observation  
 856 node is a zero-dimensional object with no volume, the crop solute uptake at each node is dimensionless.  
 857 Therefore, the crop solute uptake values per observation node are normalized (separately each for  
 858 carbamazepine and the generic tracer) to the highlighted values.

<b>Solute mass balances</b>	<b>Irrigated solute (mg)</b>	<b>Drained solute (mg)</b>	<b>Crop solute uptake (mg)</b>	<b>Crop solute uptake fraction</b>	<b>Horizontal solute discharge (mg)</b>	<b>Vertical solute discharge (mg)</b>	<b>Biodegraded solute fraction</b>
Base model (generic tracer)	16.3	0.520	1.75	0.107	12.7	0.0330	0
No regional flow model (generic tracer)	25.4	0.176	2.40	0.094	14.1	2.82	0
High regional flow model (generic tracer)	11.1	0.909	1.23	0.111	9.29	0.0037	0
Base model (Carbama zepine)	16.3	0.689	0.136	0.00833	1.46	0	0.666
No regional flow model (Carbama zepine)	25.4	0.177	0.214	0.00840	1.07	0.00116	0.707
High regional flow model (Carbama zepine)	10.9	1.03	0.0941	0.00860	1.41	0	0.672

Total root solute uptake at observation node	Directly above drain		Midway between drains	
	0.2m depth	0.6m depth	0.2m depth	0.6m depth
Base model (generic tracer)	1	0.291	0.281	0.0818
No regional flow model (generic tracer)	1.29	0.355	0.306	0.0879
High regional flow model (generic tracer)	0.678	0.211	0.188	0.0529
Base model (Carbama zepine)	1	0.663	0.0566	0.0487
No regional flow model (Carbama zepine)	1.76	1.10	0.0052	0.0056
High regional flow model (Carbama zepine)	0.558	0.349	0.0896	0.0734

859

860

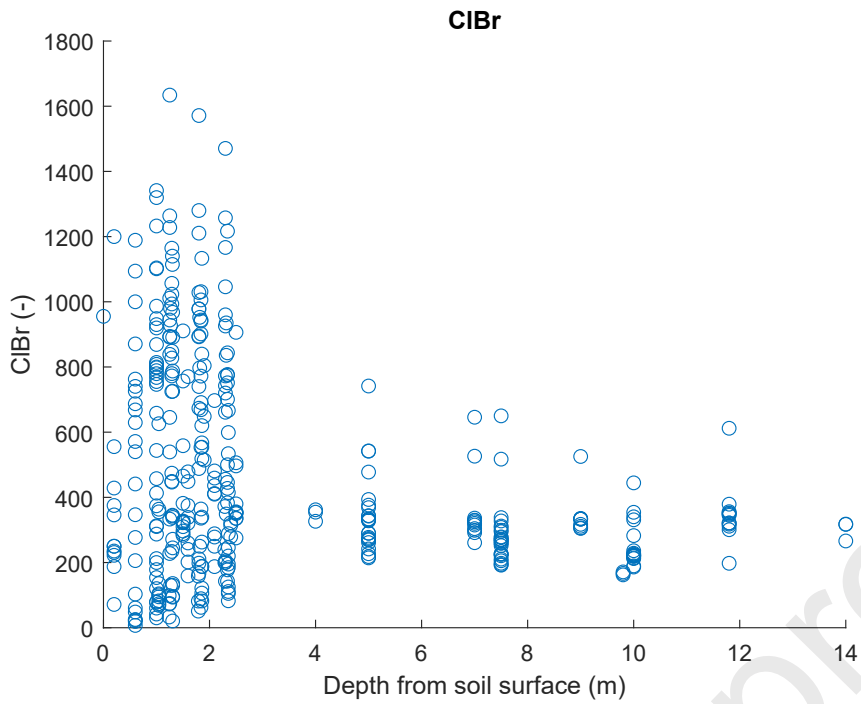


861

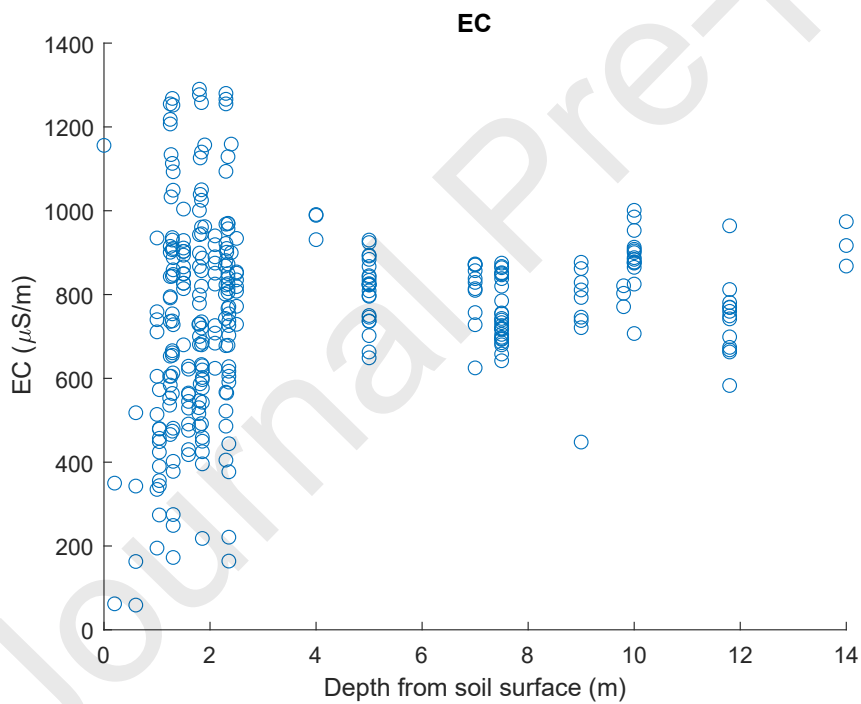
862 Figure 1: Groundwater levels from reference field data and the model without irrigation and drainage.

863

864



865 a.



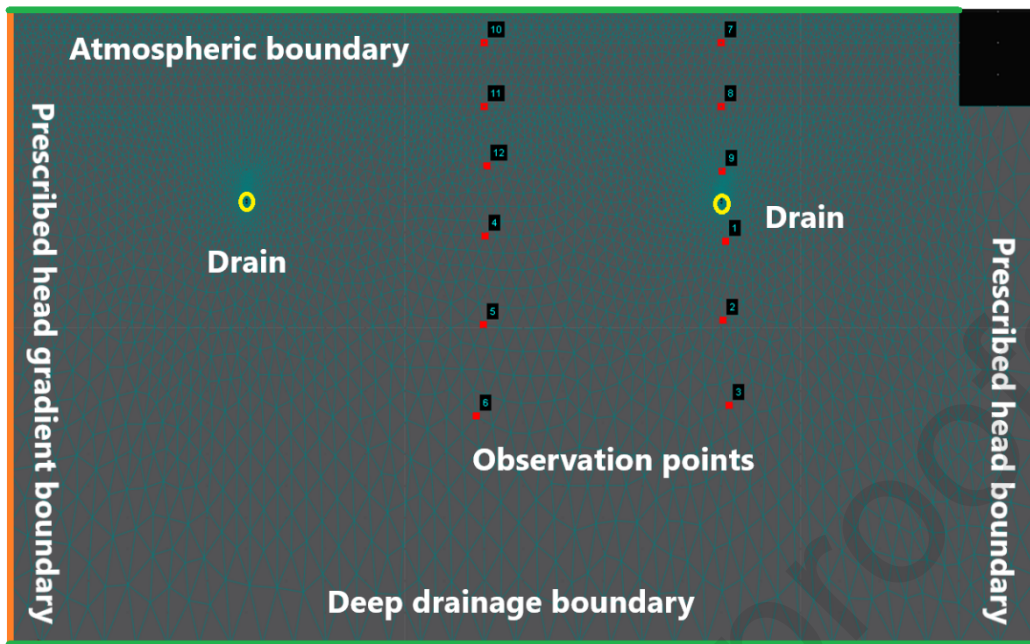
866 b.

867 Figure 2: Scatterplots of (a) Cl:Br and (b) EC of subsurface water obtained from field measurements  
868 taken at various locations and times over the experimental period.

869

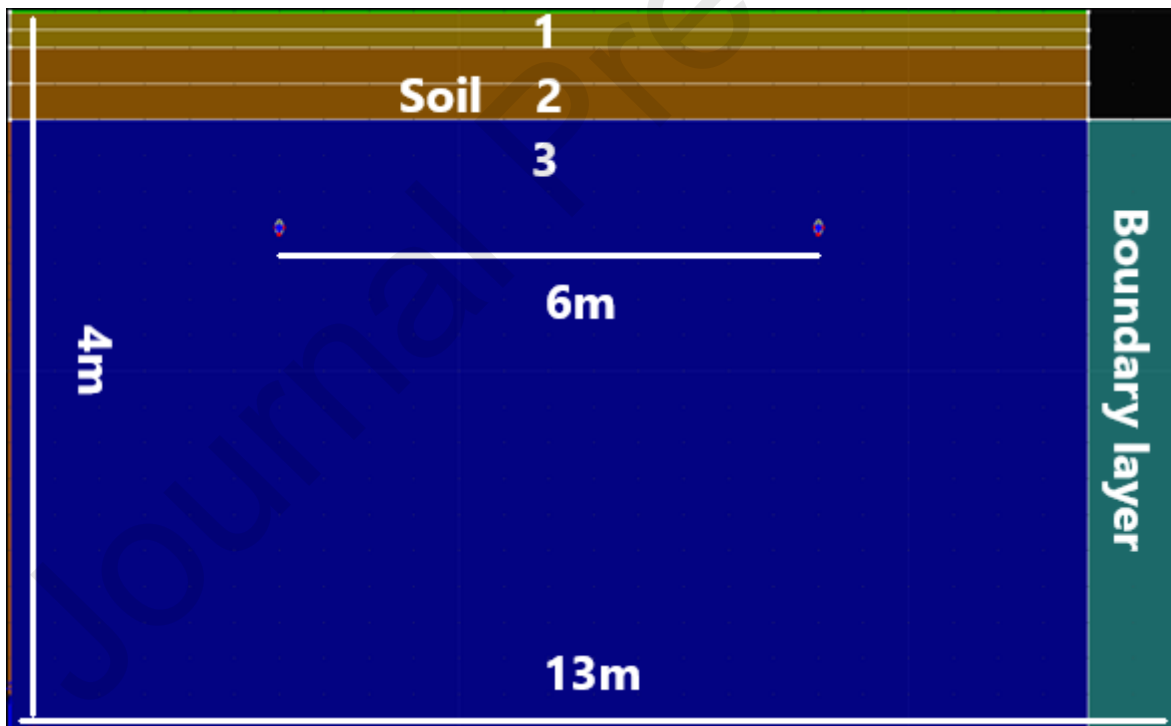
870

871 a



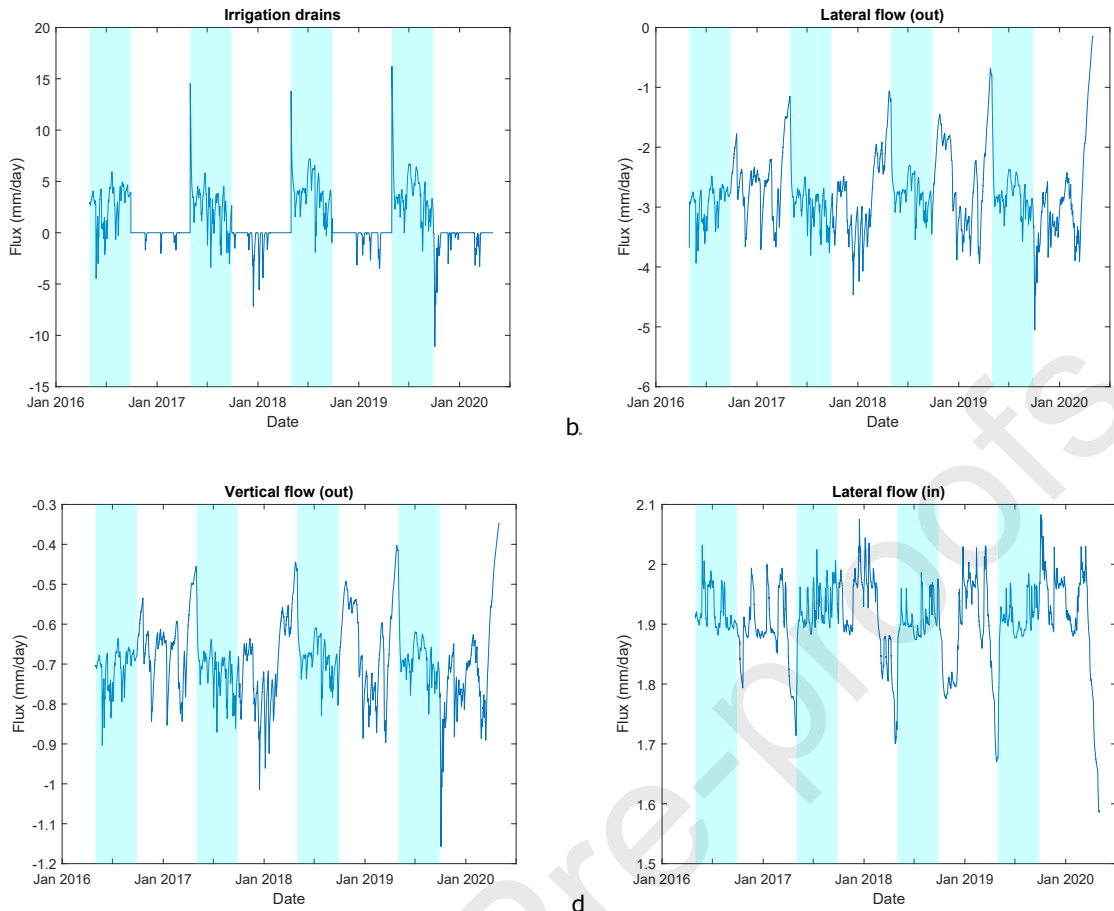
872

873 b



874

875 Figure 3: (a) Cross-section of the numerical model domain showing the locations of observation points,  
 876 the drains, and the four boundary conditions. Regional groundwater flow flows from left to right. (b)  
 877 Domain of the numerical model showing soil types and root zones. The four brown layers are the root  
 878 zone layers (Section 2.2).



879 a.

b.

880 c.

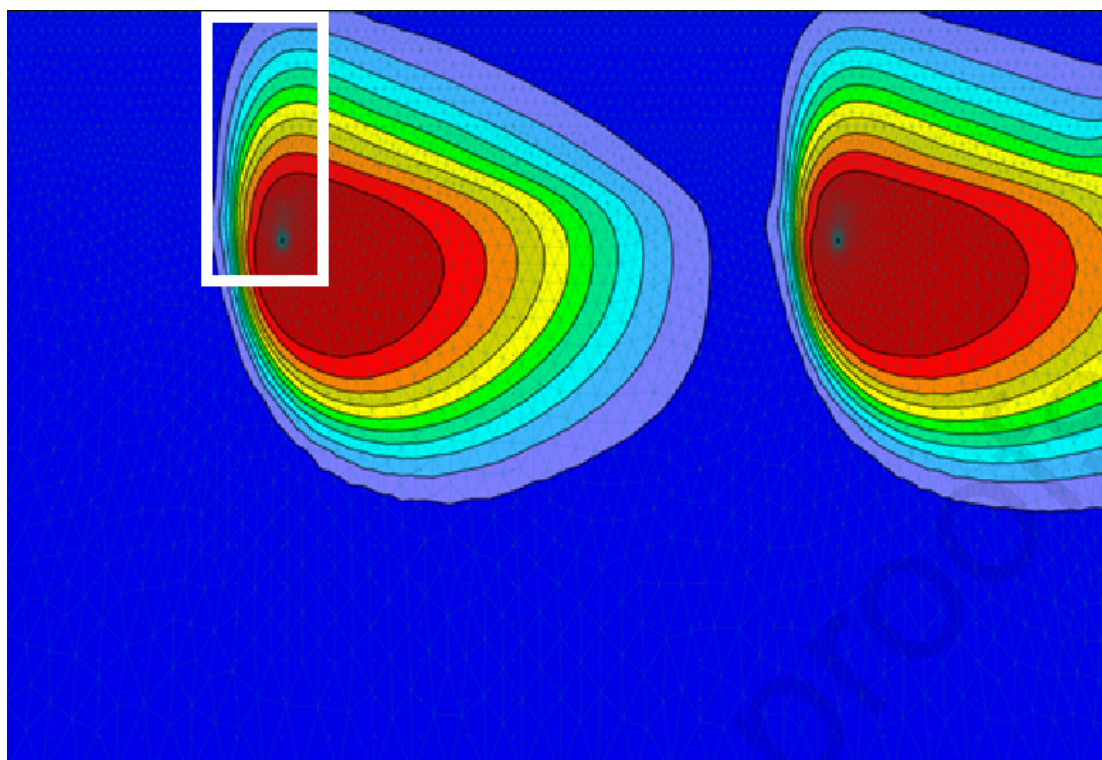
d.

881

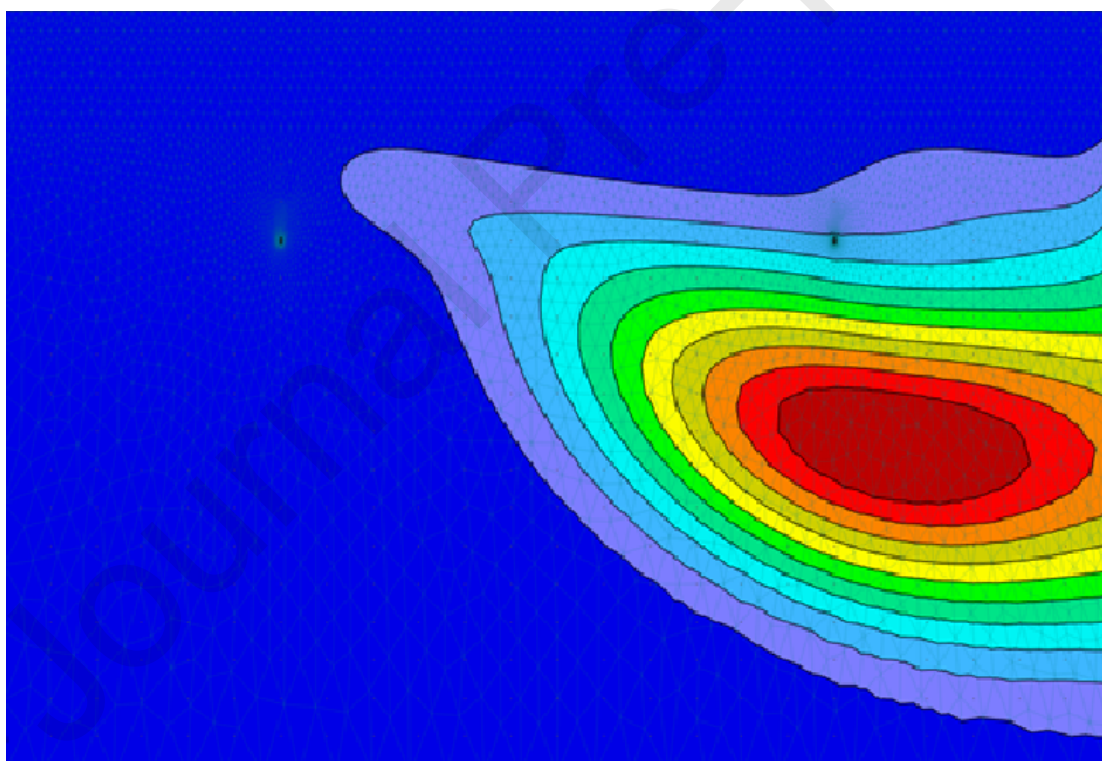
882 Figure 4: Water fluxes for the base model. Positive fluxes are fluxes into the domain, and negative fluxes  
883 are fluxes out of the domain.

884

885



886 A

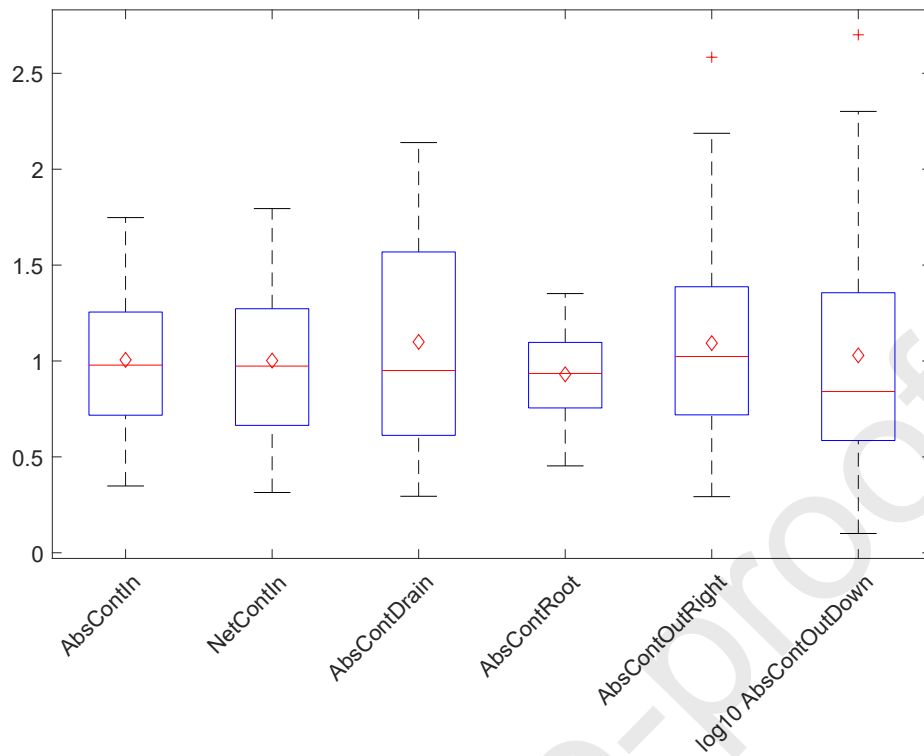


887 b

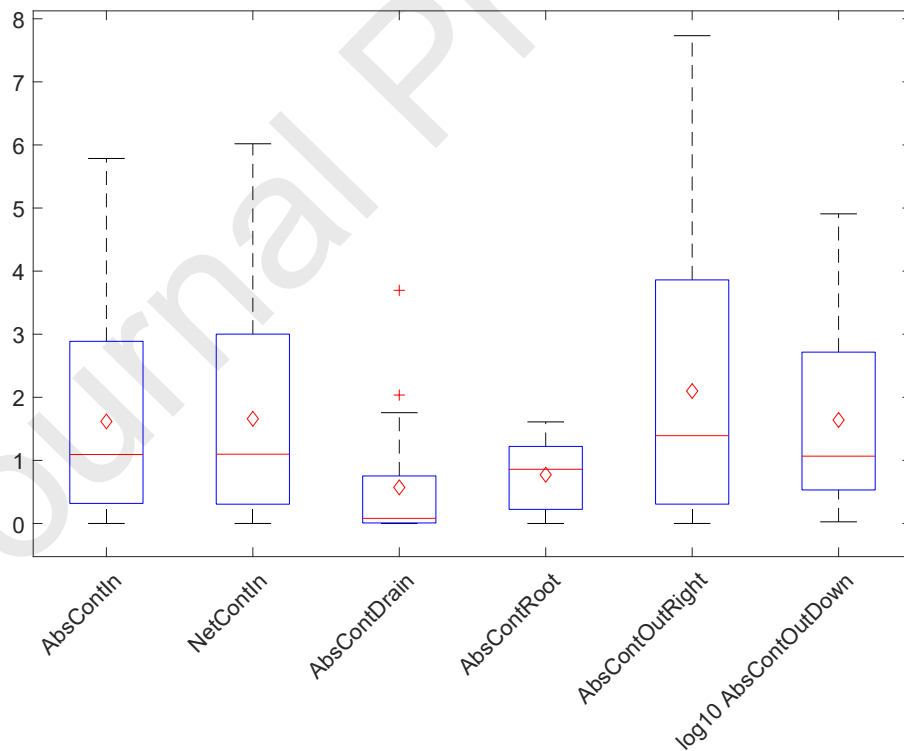
888 Figure 5: (a) Tracer plume in the base model at the end of the first crop season. The white box illustrates  
 889 approximately the area of the plume that may potentially be recovered by the drains after the crop  
 890 season. (b) Tracer plume in the base model at the end of the fourth drainage season. The plume  
 891 encompassing the drain on the right was originally injected by the drain on the left during the fourth crop  
 892 season. The continuum of colors indicate tracer concentrations, with a scale normalized to the irrigated  
 893 (red) and background (blue) concentration.

894

Journal Pre-proofs



896 a



897 b

898 Figure 6: Summary statistics boxplots of the 30 simulations with (a) weak and (b) strong spatial  
 899 heterogeneity, normalized against the values of the homogeneous base model. The boxes represent the  
 900 interquartile range, whiskers represent 1.5x interquartile range, the plusses are outliers, the red lines are  
 901 the medians, and the diamonds are means. Variable names are AbsContIn = absolute injected solute  
 902 mass; NetContIn = net injected solute mass (injected - drained), ContRoot = total root solute uptake,  
 903 AbsContDrain = absolute drained solute mass, AbsContOutRight = absolute horizontal solute discharge,

904 AbsContOutDown = absolute vertical solute discharge. Statistics of  $\log_{10}(\text{AbsContOutDown})$  are  
905 displayed because the raw AbsContOutDown data is observed to be exponentially distributed.

906 **Highlights:**

907 New subsurface irrigation and drainage method that raises the phreatic water table.

908 New method synergistic with marginal water irrigation: crops not directly exposed.

909 Tool for irrigation, freshwater conservation, and wastewater treatment and disposal.

910 Crop contamination risk is low, except by mobile contaminants in very dry years.

911 Crop and wider environmental contamination risk largest for persistent contaminants.

912

913 **CRedit authorship contribution statement**

914 Darrell Tang: Conceptualization, Formal analysis, Investigation, Methodology, Software, Writing - original  
915 draft

916 Sjoerd van der Zee: Conceptualization, Funding acquisition, Supervision, Writing - review & editing

917 Dominique Narain-Ford: Investigation

918 Ge van den Eertwegh: Investigation

919 Ruud Bartholomeus: Conceptualization, Funding acquisition, Investigation, Supervision, Writing - review  
920 & editing

921

922

923 **Abstract**

924 Managed phreatic zone recharge with marginal water, using (existing) drainage systems, raises the  
925 water table and increases water availability for crops. This is a newly developed method of freshwater  
926 conservation and marginal water treatment and disposal, but risks crop and environmental  
927 contamination. The fate of contaminants of emerging concern (CECs) within the irrigated water is  
928 addressed. We introduce numerical and analytical models, inspired loosely by a field site where treated  
929 domestic wastewater is used for subsurface irrigation. The treated wastewater would otherwise have  
930 been discharged into rivers, thereby spreading downstream. Model results show that minimal amounts of  
931 CECs are transported to deeper aquifers. Crops are not contaminated, except during dry years where  
932 small amounts of mobile CECs rise to the root zone, but then only directly above each irrigation drain.  
933 Under an annual precipitation surplus, less-mobile solutes are thus unlikely to ever enter the root zone.  
934 The primary mechanism of solute transport is lateral advection within the phreatic aquifer. Despite  
935 spatio-temporal heterogeneity in water flux magnitudes and directions, contaminant retardation does not  
936 significantly alter mass balance outcomes, only how fast it gets there. Therefore, persistent CECs pose  
937 the greatest risks, though overall environmental and crop contamination risks appear low. To maximize  
938 complementarity with subsurface irrigation systems, future advances in water treatment technologies  
939 should focus on removing persistent CECs. However, the system may be unsuitable for climates with  
940 annual precipitation shortages, as CECs may accumulate in the root zone and crops.

941